Direct observation of local resistance switching in WO_3 films

2011 J. Phys. D: Appl. Phys. 44 205302

(http://iopscience.iop.org/0022-3727/44/20/205302)

IOP PUBLISHING JOURNAL OF PHYSICS D: APPLIED PHYSICS

J. Phys. D: Appl. Phys. **44** (2011) 205302 (5pp) doi:10.1088/0022-3727/44/20/205302

Direct observation of local resistance switching in WO_3 films

C Y Dong[1,2], L Shi[1], D S Shang[1], W Chen[2], J Wang[1], B G Shen[1] and J R Sun[1]

[1] Beijing National Laboratory for Condensed Matter Physics and the Institute of Physics, Chinese Academy of Sciences, Beijing 100190, People's Republic of China

[2] Department of Physics and Hebei Advanced Thin Film Laboratory, Hebei Normal University, Shijiazhuang 050016, People's Republic of China

E-mail: jrsun@g203.iphy.ac.cn

Received 14 February 2011, in final form 30 March 2011
Published 3 May 2011
Online at stacks.iop.org/JPhysD/44/205302

Abstract

Local resistance switching in WO_3 films has been studied based on the conducting atomic force microscope technique. Special attention was paid to the formation/reproducibility of local conduction regions on the metal–oxide interface for repeated setting–resetting operations and the effects of microscopic inhomogeneity. It is found that most of the conducting spots prefer to stay where they were once formed. However, only a minority of them (∼30%) are repeatable in resistance values for the writing–erasing cycling. According to the resistance switching behaviours, five kinds of locations can be classified in total, and they are inactive regions, weak transition regions, weak to stable transition regions, stable transition regions and irregular transition regions. A further analysis shows the preferential locations of conduction spots at protuberant grains.

(Some figures in this article are in colour only in the electronic version)

1. Introduction

Electric pulse-triggered resistance switching between distinctive states of the metal–oxide–metal (MOM) structures has attracted considerable attention in recent years due to its potential application to nonvolatile memories [1–3]. A key factor affecting the practical application of this phenomenon is its reversibility for repeated writing–erasing operations. It has been experimentally revealed that conduction filaments/local regions across the insulating oxide/Schottky barrier at the metal–oxide interface form under the impact of electric field [3–5]. Obviously, it is the conduction filaments/regions that directly affect the reversibility of resistance switching.

We noted that most of the previous studies on the endurance and retention of the resistance switching have been based on macroscopic measurements. Although this provides us with valuable knowledge about the physical processes in the MOM device, the information on the formation, expansion and migration of individual conduction filaments/spots is much more important for a thorough understanding of the diverse behaviours of the electroresistance (CER) effect in the oxide-based structure. The conducting tip of the atomic force microscope (AFM) can act as a moveable electrode. It can provide the first-hand information about the physical processes at the metal–oxide interface, which has been hidden by metallic electrode in the case of macroscopic measurements. The effectiveness of this technique was demonstrated by many recent experiments, such as the direct observation of the formation/rupture of conduction filaments under the induction of electric field [6] and the field-induced resistance growth of the conductive $La_{0.7}Sr_{0.3}MnO_3$ film on the $SrTiO_3$ single crystal [7].

Tungsten oxide is an important wide band gap (2.57–3.25 eV) semiconductor with interesting physical and chemical properties, and has been widely studied for applications such as electrochromic devices, gas sensing and catalysis [8–10]. Since tungsten is used as interconnect material between different metallization levels, tungsten oxide is well compatible with the back-end-line process in the CMOS technology [11], and its application to electronic devices has been a topic of significant investigation [12, 13]. WO_3 is also a potential candidate for resistance switching. There is evidence for interface modulation-induced resistance switching in the

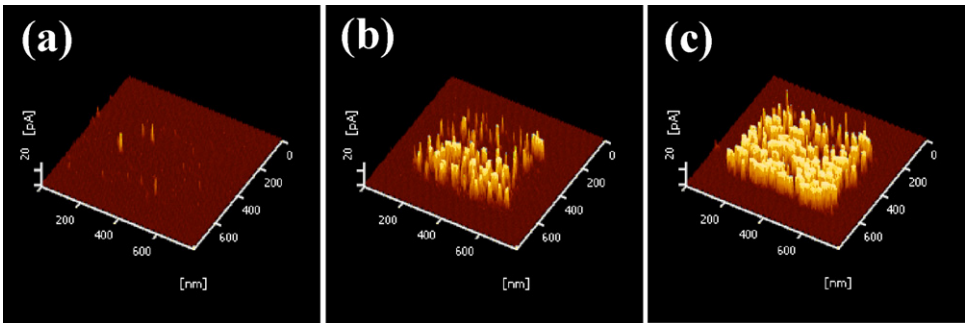

Figure 1. Current mapping after the scanning with the tip biased by the voltages of −1 V (*a*), −2 V (*b*) and −3 V (*c*). The lateral size of the images is 0.8 × 0.8 μm^2, and the current limit is 30 pA.

Au–WO_3 system [14]. In this paper, we will perform a systematic study on the CER properties of the WO_3 film grown on Pt substrates based on the conducting AFM technique. Special attention was paid to the formation/reproducibility of local conduction regions at the metal–oxide interface for repeated setting–resetting operations and the effects of microscopic inhomogeneity. It is found that most of the conducting areas preferred to stay where they were once formed though their resistances may vary with repeating writing–erasing cycling. It is further found that the film is microscopically inhomogeneous, and different resistance switching behaviours are observed at different locations.

2. Experimental procedures

The WO_3 film was grown, by the pulsed laser ablation technique (wavelength = 248 nm, repetition rate = 3 Hz and fluence = 7 J cm^{-2}), on Pt-coated Si substrate of dimensions 3 × 1 mm^2. The temperature of the substrate was kept at 400 °C, and the oxygen pressure was maintained at ∼10 Pa during the deposition. The film thickness is ∼200 nm, determined by deposition time. A post annealing at 500 °C for 5 min in O_2 flow was subsequently taken to improve the crystallinity of the film. X-ray diffraction analysis (not shown) shows that the WO_3 film is single phase and highly textured along with the preferred orientation (0 0 1).

A Nanonavi E-SWEEP SPM system (Seiko, Japan) has been employed in the present experiment. To avoid electrochemical reaction between the metallic tip and the grounded sample, all the measurements were conducted in a low humidity environment, in the atmosphere of a mixture of oxygen and nitrogen (99.99%) of a ratio of 3 : 7. The experimental procedures are as follows: first, an area of the film surface (0.5 × 0.5 μm^2) was scanned by the Au tip that is negatively biased to induce local resistance transition, then the current distribution in a slightly larger area that covers the previous one (0.8 × 0.8 μm^2) was measured under the bias voltage of 0.1 V, and, finally, an erasing operation (tip bias = 3 V) was performed to drive the sample back to its initial state. The writing–erasing cycling was repeated several times to examine the repeatability of the conduction paths. To monitor the evolution of the resistance switching, tip voltages ranging from −1 to −3 V were employed for the data writing. The AFM tip was constantly biased during the read/write operation, and the tip spends a fixed amount of time over each scanning point.

3. Results and discussions

Figure 1 shows the current distribution after the data writing under the tip voltages of −1, −2 and −3 V. In the case of low bias, most of the processed regions remain in high resistance state, and only a few locations, tens of nanometres in diameter, are activated (figure 1(*a*)). However, ∼32% of the scanned regions are modified by the scanning of −2 V, and current peaks with considerable heights can be detected (figure 1(*b*)). When the tip voltage grows to −3 V, considerable expanding and grouping of the conducting regions occur, resulting in sizable and irregular conducting islands (figure 1(*c*)). A remarkable observation is the resistance variation from location to location though the tip voltage is fixed. This is a signature of microscopic inhomogeneity of the sample, and will be discussed later.

It is worthwhile to take a close inspection of the repeatability of current spots, not only their positions but also their shapes. Figures 2(*a*)–(*d*) show four typical current mappings collected respectively after the first and third writing/erasing cycling under a fixed voltage of −2.5 V/3 V. An erasing operation deletes the current spots completely, yielding a uniform background. A quantitative analysis shows that the background current is below 0.5 pA. Current spots appear again after the rewriting operation, with their position and brightness being essentially unchanged. For a clear comparison, the image of the fifth cycling (figure 2(*e*)) has been superimposed on the first one (figure 2(*a*)), and the results are presented in figure 2(*f*). From these experimental data, three features can be identified. First, the positions of most current spots, including faint spots, are essentially unaffected by repeated operations. Changes in spot shape are also small, and the main geometric feature of the current island remains. This result confirms the hypothesis that the conduction spots prefer to stay where they were once formed. Second, visible changes occur for some faint spots. Spots at some locations, as marked by the circles in the images, fade out gradually and appear elsewhere. This is an indication for the rearrangement of conduction spots with repeated scanning. In fact, resistance could be a measure of degree of the interface modification. The latter may not be well organized when its resistance is high, and could undergo

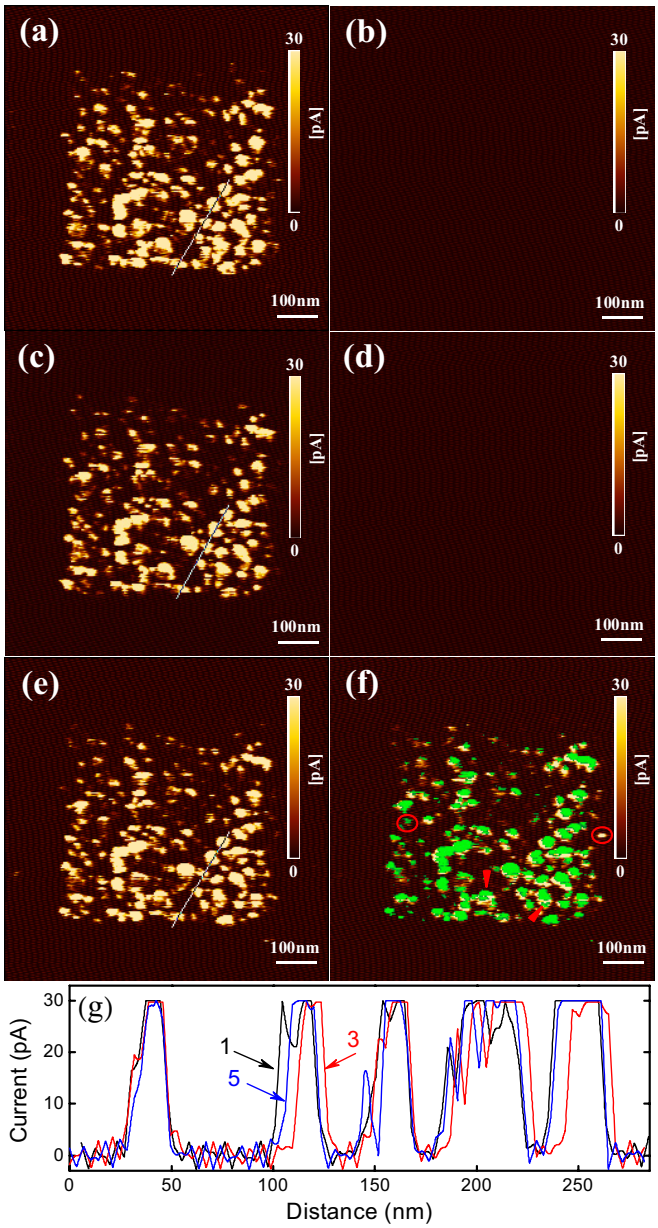

Figure 2. Typical current mappings collected after the first (*a*), (*b*) and third (*c*), (*d*) writing/erasing cycling under the tip voltage of −2.5 V/3 V, and the fifth writing operation (*e*). The comparison for the first (yellow) and fifth (green) images is shown in (*f*). The slight mismatch is due to a minor upright drift of the scanning tip. Circles mark the rearranged current spots, and split spots are marked by triangles. Line profiles across selected spots, marked by the straight line, are presented in (*g*).

a reconfiguration for repeated stimuli. Third, minor changes occur to the shape of bright spots. As shown in figure 2(*f*), some spots slightly shrink or expand, and occasionally break into pieces as marked by triangles in the image. Figure 2(*g*) presents the line profile of selected current spots. It clearly shows the reshaping of the current peaks.

In addition to reversibility, the microscopic spatial inhomogeneity deserves special attention. As proposed by the distribution of the spot brightness (figures 2(*a*), (*c*) and (2(*e*)), the local resistance may vary from place to place. The regularity of the resistance switching can be quantitatively analysed. In figure 3 we show the current oscillation against the writing–erasing cycling, obtained under the typical stimulus voltage of −2.5 V (only the current in the low resistance state is shown for clarity). Based on these data, five different behaviours can be identified in total. First, in some regions the current is very low and cannot be distinguished from noise signals (figure 3(*a*)). This actually indicates the absence of resistance transition. Second, in some places resistance switching occasionally fails, though it occurs frequently (figure 3(*b*)). This signifies the occurrence of a weak resistance transition. Third, the current experiences a low to high transition with repeating operations, and rapidly saturates at stable values (figure 3(*c*)). We will call this weak to stable transition. Fourth, the resistance switching is well reversible (figure 3(*d*)), and the resistance fluctuation in the low resistance state is generally below 50%. It will be denoted as stable transition. In this case, the current peak is usually well above 4 pA. Finally, in some regions whether the resistance transition occurs or not is totally random against the setting–resetting cycling (figure 3(*e*)).

In the first two cases a much strong stimulus may be required for a stable transition. Case three demonstrates a tendency towards stability of the conduction spots after repeated writing, which indicates the insufficiency of the stimulant voltage for these regions. Case four deserves special attention. It determines the reversibility and stability of the resistance switching, and a further analysis of its origin could be helpful for the optimization of the CER effect in oxides. These results reveal the strong irregularity of the current switching, thus the complexity of the CER effect in the WO_3 film. It could be a generic feature of oxide films due to the microscopic inhomogeneity beyond the capture of the sample deposition conditions. It should be noted that there are some locations where the current switching varies irregularly. This is the origin for the fluctuation of the resistance for repeated switching observed by macroscopic measurements. Figure 3(*f*) is the total current, the current of the stable transition, and the current of the weak to stable and irregular transitions, obtained by integrating the current over the corresponding regions. It shows that the current fluctuation mainly comes from the latter two processes.

To get a quantitative picture about the probability for each kind of resistance switching, in figure 4 we show the proportion of the regions that display different resistive behaviours. It is obvious that most of the regions are inactive under the tip voltage of −1 V. Although rare locations exhibit visible current, they are not stable for repeated scanning. When the tip voltage increases to −2 V, the population of the regions of the weak and weak to stable transition grows rapidly, at the expense of the resistive regions. However, stable switching is still rare. The stable transition is significantly enhanced by a further increase in tip voltage (−2.5 V), as demonstrated by the steep growth of its population from ∼5% to ∼29.5%. Correspondingly, the proportion of weak to stable regions reduces, an indication of the occurrence of an unstable–stable transition. This is understandable noting the fact that the increase in activation voltage could have a similar effect as repeating stimuli. The growth of irregular transition

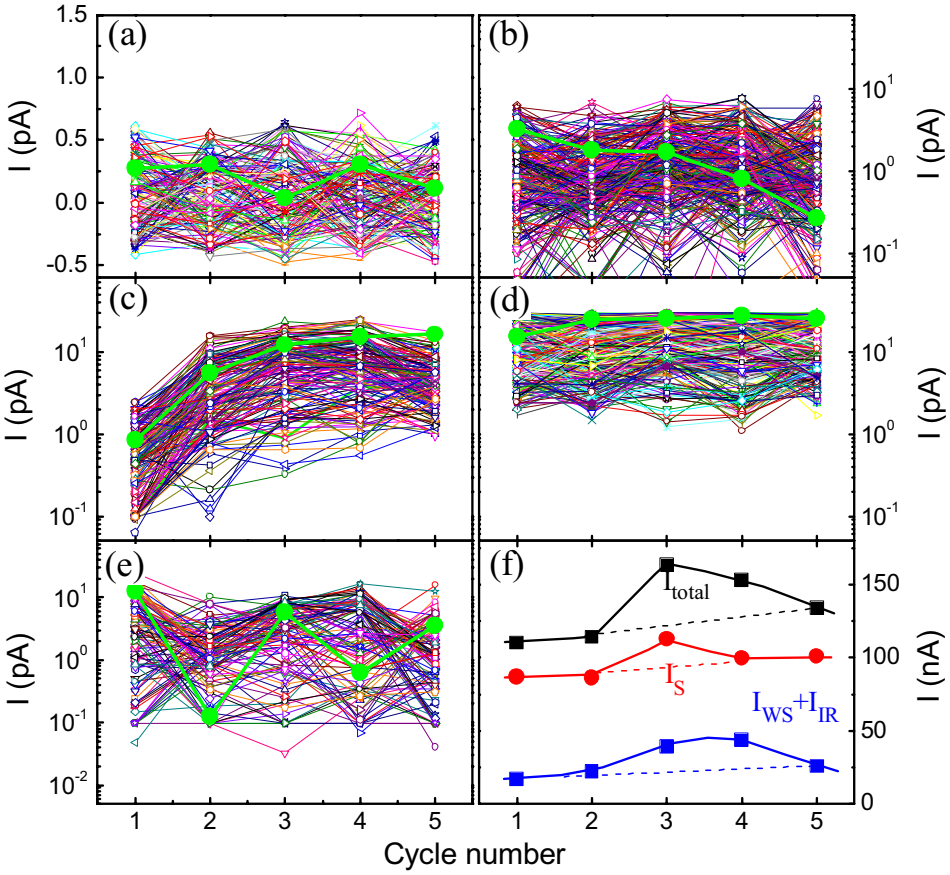

Figure 3. Variation of current with repeated writing–erasing operations, recorded after the typical stimulus voltage of −2.5 V (only the low resistance current is show for clarity). Five different switching behaviours marked by non-transition (*a*), weak transition (*b*), weak to stable transition (*c*), stable transition (*d*) and irregular transition (*e*) can be classified. The total current, the currents for stable and weak to stable and irregular transitions are shown in (*f*), obtained by integrating the current over the corresponding areas. The bold curve in each figure marks the typical current variation. Each curve in (*a*)–(*e*) comes from a single location in the sample.

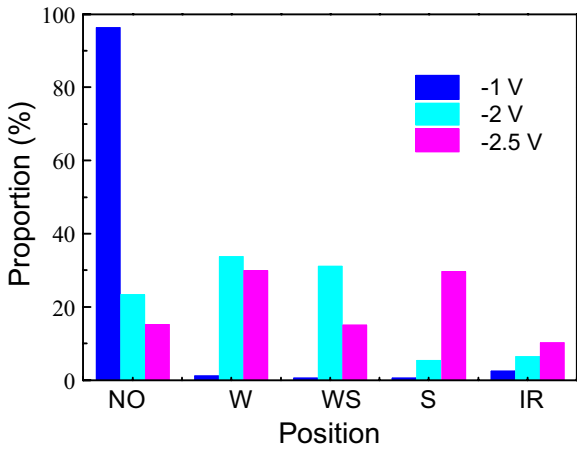

Figure 4. Proportion of the regions showing different resistance switching. Labels in the figure have the following meanings: NO: non-transition, W: weak transition, WS: weak to stable transition, S: stable transition, IR: irregular transition.

regions indicates the presence of a voltage window for a stable transition.

It is instructive to examine the correlation between film morphology and current distribution. Figure 5(*a*) is a comparison of film morphology and current distribution, the latter is obtained under the bias voltage of −1 V. Figure 5(*b*) presents the line profiles of the current mapping and film morphology. It shows that the significant current prefers to appear within the grains, whereas gain boundaries are relatively insensitive to electric field. The latter could be ascribed to the interfacial barrier because of the charge accumulation/depletion at the grain boundaries, and may be an origin for microscopic inhomogeneity. The influence of surface roughness on resistance switching is also an issue deserving attention. For the WO_3 film, the AFM analysis shows that the root-mean-square roughness is ∼2 nm, the lateral grain size is ∼80 nm, and the peak-to-valley height is ∼10 nm (not shown). For simplicity, six grain ranges, with the outcrops below 5 nm, 5–6 nm, 6–7 nm, 7–8 nm, 8–9 nm and above 9 nm, have been classified. A direct statistics gives the probability for a bright current spot (>30 pA) locating at the grain (figure 5(*c*)). It seems that the resistance transition prefers to appear at protuberant grains. This result is consistent with our previous observation that film roughness has a strong effect on resistance switching for the $La_{0.67}Sr_{0.33}MnO_3$ film [15].

As summarized above, there are in total five different regions that can be classified based on their switching behaviours. Noting the large probability of the current spots on the gibbous grains, stable switching may prefer to occur on

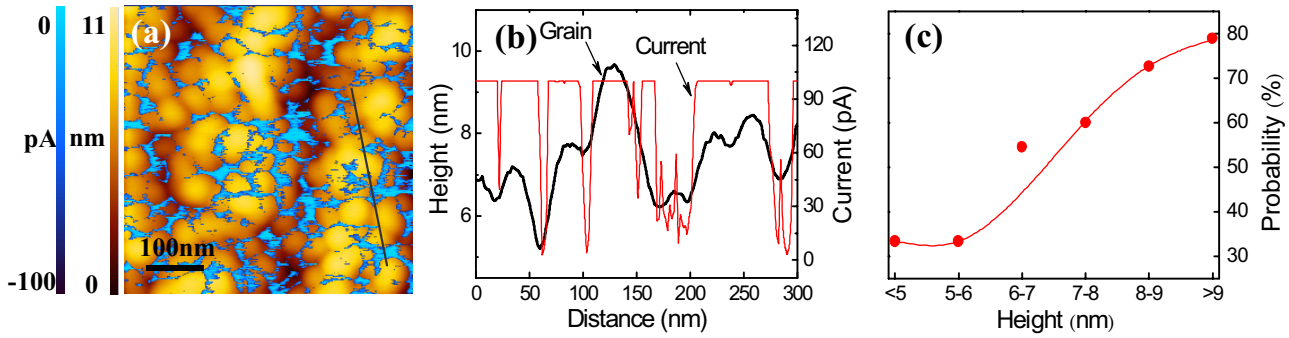

Figure 5. Correlation between resistance transition and film morphology. (*a*) A comparison of film morphology and current mapping acquired under the bias voltage of −1 V. (*b*) Line profiles of the current mapping (current limit is 100 pA) and film morphology extracted along the line marked in (*a*). (*c*) Probability for the current spots (>30 pA) located at different grains.

these grains, probably due to their different microstructures and chemical compositions from other locations as discussed later. In contrast, the inactive regions may mainly situate around grain boundaries. Corresponding to the transition from the protuberant grains to the grain boundaries, the activeness of the oxide surface evolves, giving rise to the intermediate regions of weak transition, weak to stable transition and irregular transition.

The variation in film thickness can cause a change in the electric field in the film. The average film thickness is ∼200 nm. A rough estimation indicates that the maximal field change is lower than ∼5%. This cannot explain the preferential location of the filaments at the protuberant grains. It has been well documented that the growth mode of the film can affect lattice defects and strains. For example, the lattice strains in the grains are generally different from those around the grain peripheries. Defects associated with the aggregation of W and O vacancies could also be different for the hollow and extruded parts of the films. This may be an origin to the different behaviours of the outcrop-dependent resistance switching. The present work suggests the importance of a careful control of film surface.

4. Summary

In summary, local resistance switching in WO_3 films has been studied based on the conducting atomic force microscope technique. Special attention was paid to the formation/reproducibility of local conduction regions on the metal–oxide interface for repeated setting–resetting operations and the effects of microscopic inhomogeneity. It is found that most of the conducting spots prefer to stay where they were once formed. However, only a minority of them (∼30%) are repeatable in resistance values for the writing–erasing cycling. According to the resistance switching behaviours, five kinds of locations can be classified in total, and they are inactive regions, weak transition regions, weak to stable transition regions, stable transition regions and irregular transition regions. A further analysis shows the preference of the conduction spots to protuberant grains.

Acknowledgments

This work has been supported by the National Basic Research of China, the National Natural Science Foundation of China, the Knowledge Innovation Project of the Chinese Academy of Science, the Beijing Municipal Nature Science Foundation.

References

[1] Beck A, Bednorz J G, Gerber C, Rossel C and Widmer D 2000 *Appl. Phys. Lett.* **77** 139
[2] Liu S Q, Wu N J and Ignatiev A 2000 *Appl. Phys. Lett.* **76** 2749
[3] Waser R, Dittmann R, Staikov G and Szot K 2009 *Adv. Mater.* **21** 2632
[4] Sim H, Choi D, Lee D, Seo S, Lee M-J, Yoo I-K and Hwang H 2005 *IEEE Electron Device Lett.* **26** 292
[5] Shang D S, Sun J R, Shi L and Shen B G 2008 *Appl. Phys. Lett.* **93** 102106
[6] Szot K, Speier W, Bihlmayer G and Waser R 2006 *Nature Mater.* **5** 312
You J and Shin Y H 2008 *Appl. Phys. Lett.* **92** 222106
[7] Moreno C, Munuera C, Valencia S, Krorian F, Pbradors X and Ocal C 2010 *Nano Lett.* **10** 3828
[8] Ho C H, Lai E K, Lee M D, Pan C L, Yao Y D, Hsieh K Y, Liu R and Lu C Y 2007 *IEEE Symp. on VLSI Technology (Kyoto)* Digest of Technical Papers, pp 228–9
Ho C-H *et al* 2010 *Int. Electron Devices Meeting (San Francisco, CA)* Technical Digest 19.1.1-4
[9] Kozicki M N, Gopalan C, Balakrishnan M, Park M and Mitkova M 2004 *Proc. 2004 Non-Volatile Memory Technology Symp. (Orlando, FL)* pp 10–14
[10] Miyake K, Kaneko H, Sano M and Suedomi N 1984 *J. Appl. Phys.* **55** 2747
[11] Granqvist C G 2000 *Sol. Energy Mater. Sol. Cells* **60** 201
[12] Siciliano T, Tepore A, Micocci G, Serra A, Manno D and Filippo E 2008 *Sensors Actuators* B **133** 321
[13] Wachs I E, Kim T and Ross E I 2006 *Catal. Today* **116** 162
[14] Shang D S, Shi L, Sun J R, Shen B G, Zhuge F, Li R W and Zhao Y G 2010 *Appl. Phys. Lett.* **96** 072103
[15] Xie Y W, Sun J R, Wang D J, Liang S and Shen B G 2006 *J. Appl. Phys.* **100** 033704